Synthesis of Metal Nanoparticles by Microorganisms

Yugo Kato and Michio Suzuki *

Department of Applied Biological Chemistry, Graduate School of Agricultural and Life Sciences,
The University of Tokyo, 1-1-1 Yayoi, Bunkyo-ku, Tokyo 113-8657, Japan; katoh.yugo@gmail.com
*   Correspondence: amichiwo@mail.ecc.u-tokyo.ac.jp; Tel.: +81-3-5841-5156

Abstract: Metal nanoparticles (NPs), with sizes ranging from 1–100 nm, are of great scientific interest because their functions and features differ greatly from those of bulk metal. Chemical or physical methods are used to synthesize commercial quantities of NPs, and green, energy-efficient approaches generating byproducts of low toxicity are desirable to minimize the environmental impact of the industrial methods. Some microorganisms synthesize metal NPs for detoxification and metabolic reasons at room temperature and pressure in aqueous solution. Metal NPs have been prepared via green methods by incubating microorganisms or cell-free extracts of microorganisms with dissolved metal ions for hours or days. Metal NPs are analyzed using various techniques, such as ultraviolet-visible spectroscopy, electron microscopy, X-ray diffraction, electron diffraction, energy-dispersive X-ray spectroscopy, and X-ray photoelectron spectroscopy. Numerous publications have focused on microorganisms that synthesize various metal NPs. For example, Ag, Au, CdS, CdSe, Cu, CuO, Gd_2O_3, Fe_3O_4, PbS, Pd, Sb_2O_3, TiO_2, and ZrO_2 NPs have been reported. Herein, we review the synthesis of metal NPs by microorganisms. Although the molecular mechanisms of their synthesis have been investigated to some extent, experimental evidence for the mechanisms is limited. Understanding the mechanisms is crucial for industrial-scale development of microorganism-synthesized metal NPs.

Keywords: biosynthesis; metal adsorption; metal nanoparticles; microorganisms

1. Introduction

Nanomaterials are of great scientific and commercial interest. Metal nanoparticles (NPs) range in size from about 1–100 nm. Their functions and features differ from those of bulk metals. Notably, the large surface area-to-volume ratio of metal NPs increases opportunities for interactions with other molecules [1]. For example, metal NPs can have antimicrobial, anticancer, catalytic, magnetic, and optical activities and thus have applications in various fields such as medicine, environmental science, and energy [2–4]. The energy state of metal NP electrons differs from that of bulk metals because of the very small particle size. This phenomenon is called the quantum size effect, and it affects the thermal, electromagnetic, and engineering properties of NPs.

Catalytic activity has been reported for Au, Ag, Pd, and Pt NPs. The color of solutions of Au and Ag NPs changes with particle size due to surface electrons that induce surface plasmon resonance (SPR). A solution of Au NPs is red or purple, while that of Ag NPs is yellow or orange. The latter are used in bactericidal, electrical, and medical products, such as for the treatment of skin diseases [5]. Au NPs attach to DNA fragments, and hence are used to diagnose viral infections [6]. Catalysts and sensors use Pd NPs. For example, Pd NPs are catalysts for Heck and Suzuki reactions [7] and can be used to detect oxygen [8] and formaldehyde [9]. A synergy between Au NPs and Pd NPs is found in core-shell Au-Pd NPs [10], which exhibit catalytic activity toward various reactions, such as oxidation of CO, alcohols, and phenols [11–13]. Pt NPs have antioxidant activities. Pt NPs can act as scavenger

for superoxide anion radical and hydroxyl radical [14]. Cu NPs are also active as gas-phase catalysts, photocatalysts, and electrocatalysts [15]. TiO_2 (Titania) NPs are used in sunscreens because they block ultraviolet (UV) light [16]. They also find applications in cancer chemotherapy and gene delivery because Ti(IV) binds to transferrin in human serum [17]. Gd_2O_3 NPs are superparamagnetic and have high dielectric constants; they are used as imaging agents in magnetic resonance imaging and as phosphors for absorption materials in atomic reactors [18]. Magnetic NPs have many applications. Notably, Fe_3O_4 (magnetite) NPs have been used in biomedical applications, such as for anticancer, antitumor, and cell labelling [19]. ZrO_2 (zirconia) NPs have high dielectric permittivity, useful optical properties, excellent thermal stability, and chemical inertness. Consequently, they are found in various electronic devices including electrodes, solar cells, and transparent thin films [20]. Semiconductor NPs are called quantum dots. These materials exhibit fluorescence (FL) enhancement that varies with particle size. CdSe NPs, which is a II–VI semiconductor with a hexagonal wurtzite structure, are used in various fields such as optical devices, electronic engineering, and catalysis. They are used in bioimaging to analyze the behavior of cells and molecules in living organisms, and as light-absorbing materials to increase the energy absorption efficiency of solar cells. CdS NPs, which is also a II–VI semiconductor, have many interesting properties [21]. Quantum dots of PbS, ZnS, and PbSe are used in optoelectronics [22], solar cells [23], and imaging [24].

Chemical and physical methods are used for large-scale synthesis of NPs. For example, Au NPs are prepared by reacting Au ions with citric acid at high temperature and pressure [25]. CdS NPs are prepared by heating dimethylcadmium with sulfur at 300 °C in an organic solvent such as trioctylphosphine [26]. These methods, which require high pressures, high temperatures, toxic chemical reagents, and organic solvents, are not environmentally friendly, so it is highly desirable to develop new methods that involve low financial and energy costs, and do not generate unwanted byproducts. One popular approach involves the biosynthesis of metal NPs using microorganisms.

Considerable research has explored the relationship between microorganisms and metals. Magnetic bacteria (*Spirochaeta plicatilis*) with magnetosomes were discovered in 1975 [27]. Magnetosomes contain Fe_3O_4 or Fe_3S_4 NPs. Magnetotactic bacteria use these NPs as compasses to detect geomagnetism. Their crystalline polymorphs depend on the bacterial species. Microorganisms produce metal NPs as a survival strategy. Microorganisms can be used to synthesize metal NPs, and there have been many reports of this being accomplished either intra- or extracellularly. Bacterial syntheses of metal NPs are ecofriendly because the processes do not require organic solvents and generate minimal waste at ambient temperature and pressure. Transmission electron microscopy (TEM) images of various metal NPs synthesized by microorganisms are shown in Figure 1.
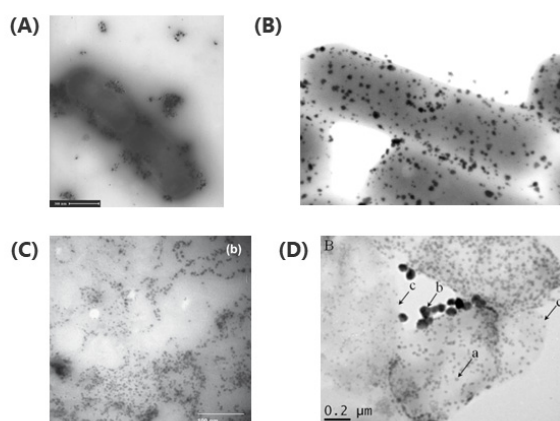

Figure 1. TEM image of microbial synthesized nanoparticles (NPs). (**A**) Ag NPs [28], (**B**) Au NPs [29], (**C**) CdS NPs [18], (**D**) CdSe NPs [30]. Reproduced with permission from Korbekandi, H. et al., Journal of Chemical Technology & Biotechnology; published by Wiley, 2012; Prasad, K. and Jha, A.K., Journal of Colloid And Interface Science; published by ELSEVIER, 2010; Ayano, H. et al., Journal of Bioscience and Bioengineering; published by ELSEVIER, 2015.

NPs containing a zero-valent metal typically require reducing agents for their synthesis. Dispersants must also be used to inhibit particle aggregation. However, most reports of NP synthesis by microorganisms have not provided clear experimental evidence of the organic molecules in microorganisms that function as reductants or dispersants. The identification of the reductants and dispersants is essential to improve the efficiency of metal NP synthesis.

There are two forms of metal NPs synthesis by microorganisms: Outside the cell and inside the cell. When metal NPs were synthesized outside the cells, the extracellular components acted as dispersants; dispersant-capped metal NPs were not aggregated. When the metal NPs synthesized outside the cells were zero-valent metals, the extracellular components and added electron donor or membrane components acted as reductants (Figure 2). However, when metal NPs were synthesized inside the cells, proteins or peptides acted as dispersants. When metal NPs synthesized inside the cells were zero-valent metals, reductants in the cytoplasm provided electrons to the metal ions (Figure 3).
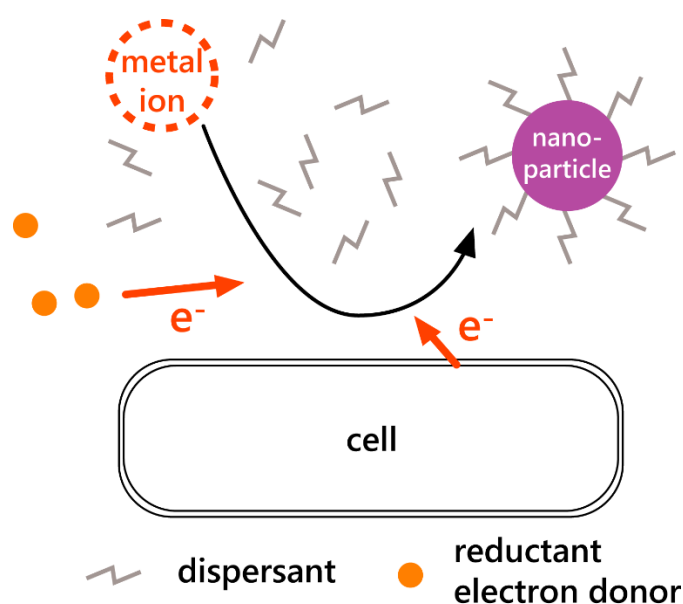

Figure 2. Model of metal nanoparticle synthesis outside cells. Metal ions are reduced by an added electron donor or reductant secreted from the cells. The secreted metabolites outside the cells surround the surface of the NPs and behave as dispersants.
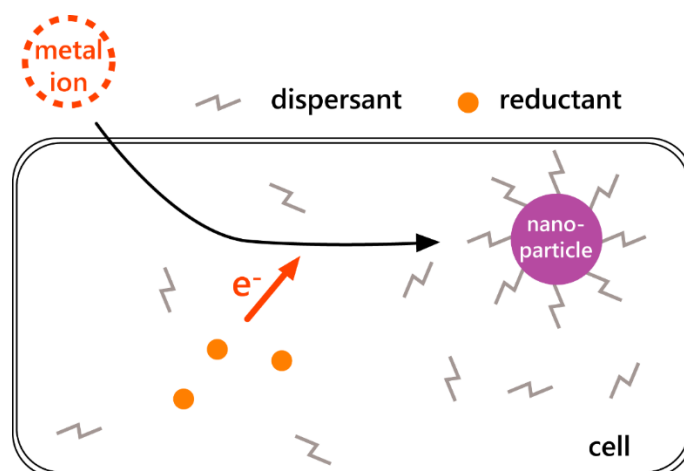

Figure 3. Model of metal nanoparticle synthesis inside cells. Metal ions are reduced by redox enzymes in the cytoplasm. The metabolites inside the cells surround the surface of NPs and behave as dispersants.

There are two reasons why microorganisms synthesize metal NPs. One reason is to protect themselves from the toxicity of metal ions. Heavy metals are toxic to microorganisms because they inhibit the function of metal enzymes and lead to the generation of reactive oxygen species. Microorganisms use various mechanisms to detoxify heavy metals, e.g., exclusion from cells using transporters, intra-cellular sequestration in vacuoles, and enzymatic detoxification using redox enzymes [31]. The detoxified metals are precipitated as minerals or are preserved in the cells as metal ions [32]. Another reason is to acquire energy; some bacteria use metal ions as electron acceptors [33].

Biosynthetic NPs are prepared by incubating cells with metal salt solutions over periods of minutes to days. Electron donors are sometimes added to the solutions (Figure 4A). To minimize the effects of culture media, cells are washed with sterile water before incubation with metal salt solution to completely remove the culture medium (Figure 4B). Secretions (cell-free extracts (CFEs)) from microorganisms have also been used for the synthesis of metal NPs. Cultured cells were incubated in sterile water for several days, and then the suspension was filtered to obtain the CFE, which was finally mixed with dissolved metal ions in vitro (Figure 4C).
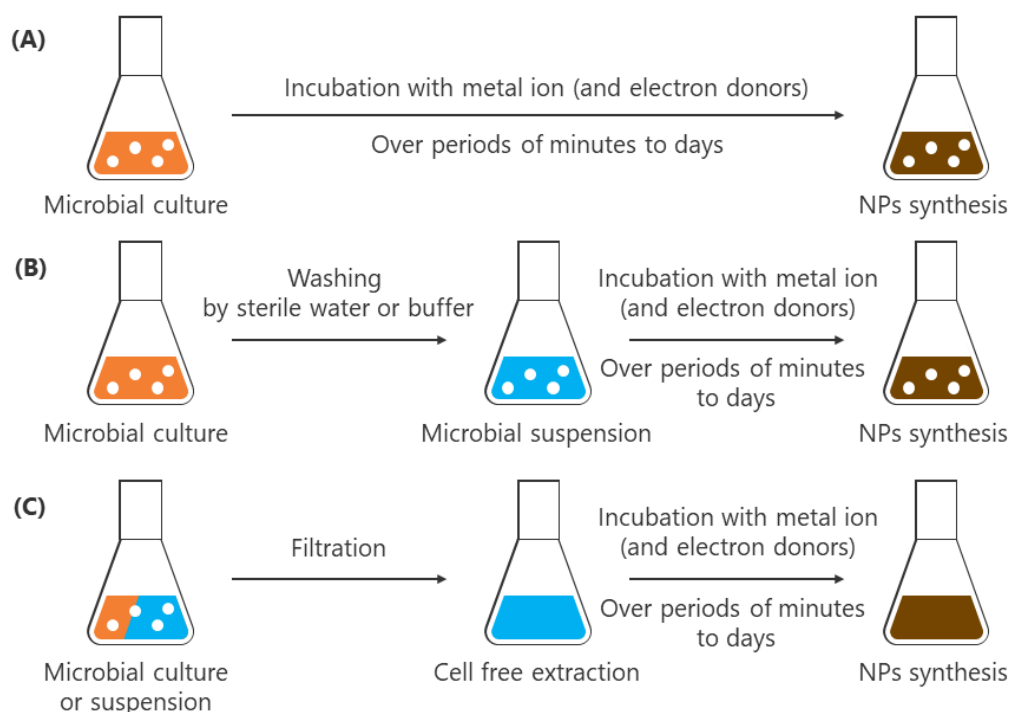

Figure 4. Scheme of metal NPs synthesis by microorganisms, (**A**) NPs synthesis by microbial culture (**B**) NPs synthesis by washed microbial culture, and (**C**) NPs synthesis by cell free extracts (CFE).

Various techniques are used to study the properties of metal NPs. These include TEM, scanning electron microscopy (SEM), energy-dispersive X-ray spectroscopy (EDS), UV-visible (UV-vis) spectrometry, FL spectrometry, dynamic light scattering (DLS), X-ray diffraction (XRD), and X-ray photoelectron spectroscopy (XPS).

TEM and SEM provide details about the shape, size, and localization of metal NPs [34,35], while EDS reveals their elemental composition [36]. As noted above, some solutions of noble-metal NPs are distinctly colored. Ultraviolet-visible [17] and FL spectroscopies are also used to characterize metal NPs such as size and shape. The wavelength of an absorption maximum depends on the NP particle size and metal species. The size distribution of metal NPs can be determined by DLS techniques [37], while XRD is used to identify crystalline polymorphs, and with the use of Scherrer's equation, this can yield estimates of their average size [19]. XPS provides details of the chemical bonding state of metal NPs [38].

This review summarizes the NPs synthesis by microorganisms in terms of biomineralizaion of microorganisms. Although many previous reviews about metal NPs by microorganisms focused on the species of microorganisms, our review categorizes the kinds of metals. We summarize reports of NPs synthesis by microorganisms in Section 2. We also note that the molecular mechanisms of metal NPs synthesis in microorganisms are important to increase the efficiency of metal NPs synthesis. The metabolites related to the molecular mechanisms reported in many publications are introduced in Section 3. As it is better to cultivate easily the microorganisms for use of application, this review shows only the microorganisms that grew in general medium and under normal temperature and pressure. Microorganisms such as anaerobes, thermophiles, acidophiles, alkaliphiles, halophiles, and polyextremophiles do so-called extreme conditions are not referred in this review.

2. Nanoparticle Synthesis by Microorganisms

2.1. Silver Nanoparticles

Table 1 lists the strains of microorganism that have been used for the synthesis of Ag NPs and the techniques used for their study.

Table 1. List of microorganisms for synthesis of Ag nanoparticles and technique for confirmation of Ag nanoparticles.

Metal	Microorganism	Classification	Active Molecules	Size (nm)	Techniques Used for Detection	Ref.
Ag	*Pseudomonas stutzeri* AG259	bacteria		20–100	TEM, UV-vis	[34]
Ag	*Fusarium oxysporum*	fungi		5~15	TEM, UV-vis	[39]
Ag	*Lactobacillus casei* subsp. *Casei* DSM 20011	bacteria		25–50	TEM, UV-vis	[28]
Ag	*Escherichia coli* K12	bacteria	hemiacetal groups of sugars	10–30	TEM, EDS, UV-vis, XPS	[36]
Ag	*Lactobacillus acidophilus* 58p	bacteria		ca. 30.7	TEM, UV-vis	[40]
Ag	*Lactobacillus plantarum* 92T	bacteria		ca. 20.0	TEM, UV-vis	[40]
Ag	*Lactobacillus delbrueckii* subsp. *Bulgaricus*	bacteria		1.4–8.9	TEM, UV-vis, XRD	[41]

Pseudomonas stutzeri AG259 bacterium, which was isolated from a silver mine, accumulated silver by forming Ag-containing NPs. Triangular, hexagonal, and spheroidal NPs were observed by TEM. UV-vis spectrum showed optical function of Ag-containing nanoparticles [34].

Fusarium oxysporum synthesized Ag NPs. An AgNO$_3$ solution was added to a suspension of *F. oxysporum* in the dark. The selected-area diffraction (SAED) pattern of the NPs revealed that the Ag particles were crystalline [39].

Lactobacillus casei subsp. *casei* (DSM 20011) also synthesized Ag NPs. An AgNO$_3$ solution was added to *L. casei* cells with glucose. The optimal synthetic conditions were as follows: 4.64 g/L of biomass, 56 mmol/L of glucose as an electron donor, and 0.1 mmol/L of AgNO$_3$ [28].

Ag NPs were also synthesized by adding AgNO$_3$ to an *Escherichia coli* K12 culture solution. Lattice-fringe fingerprinting of Ag NPs was completed using high-resolution TEM (HR-TEM) [36].

Garmasheva et al. reported the synthesis by certain *Lactobacillus* species. Ag NPs were prepared by incubating cells washed by sterile water with AgNO$_3$. The Ag NPs synthesized by *L. acidophilus* 58p

and by *L. plantarum* 92T exhibited antimicrobial activity. Moreover, NPs synthesized by *L. acidophilus* 58p were more active than *L. plantarum* 92T against some bacteria [40].

Extracts of *Lactobacillus delbrueckii* subsp. *Bulgaricus* isolated from kindrimo (locally fermented milk) from settlements of Fulani nomadic herdsmen of Kano State, Nigeria were used to prepare Ag NPs. Under sunlight irradiation, the *L. delbrueckii* extract was mixed with $AgNO_3$ solution. Sunlight irradiation was essential for the synthesis [41].

2.2. Au Nanoparticles

Table 2 lists the microorganism strains used for the synthesis of Au NPs and the techniques used for their study.

Incubating *Verticillium* sp. (AAT-TS-4) with $HAuCl_4$ formed Au NPs. TEM observations of thin sections of the cells revealed that the NPs were present on the cell wall (outer boundary) and on the cytoplasmic membrane [7].

Au NPs were also synthesized using *Rhodococcus* sp. and an alkalotolerant actinomycete. The bacterium was isolated from fig trees from the Pune district of Maharashtra, India. TEM of ultrathin sections of cells containing the Au NPs established that the particles were located in the cell wall and the cytoplasmic membrane. Notably, there were more NPs in the cytoplasmic membrane. Biosynthesis of the Au NPs did not hinder bacterial multiplication [35].

Au NPs were also synthesized on the surface of *E. coli* DH5α. TEM observations revealed that the NPs were mostly spherical [42].

Rhodopseudomonas capsulate was also used to synthesize Au NPs. The synthesis was pH-dependent, and spherical Au NPs were observed at pH 7 by TEM [43]. Furthermore, CFEs from *R. capsulate* also synthesized Au NPs. The shape of the NPs depended on the Au ion concentration. At lower concentrations, spherical Au NPs were synthesized, while Au nanowires were synthesized at higher concentrations [44].

Au NPs were synthesized by *Shewanella algae*, which is an iron-reducing bacterium. The synthesis was very rapid, with reduction of gold ions occurring within 30 min. The similarity of the reduction potentials of the Fe(III) and noble-metal ions enabled the synthesis of the Au NPs [33,45].

Au NPs were synthesized using the culture supernatant of *Aspergillus niger* NCIM 616. The mycelial mass of *A. niger* NCIM616 was washed with Milli-Q water and incubated in deionized water. The culture supernatant was obtained by filtration. TEM revealed that adding $AuCl_3$ solution to the culture supernatant produced NPs [46].

Cupriavidus metallidurans CH34, which forms biofilms on Au grains, accumulated Au(III) complex. Synthesized Au NPs were located in the cytoplasm, suggesting cytoplasmic reduction. Micro X-ray FL analysis established that the NPs were localized within the cell envelope [47].

High-resolution TEM observations revealed that Au NPs with an average diameter of 10 nm were synthesized by incubating a suspension of *Rhizopus oryzae* MTCC 262 with $HAuCl_4$. The particles were located on the cell membrane. Atomic force microscopy (AFM) revealed morphological changes of the nanogold-bioconjugate (NGBC) after adsorption of organophosphorus pesticides. This NGBC also exhibited highly antibacterial activity [48].

Au nanocubes were synthesized using *Bacillus licheniformis*. The nanocubes observed by SEM ranged in size from 10–100 nm. Based on UV-vis spectroscopy and XRD, their average diameter was determined to be 67 and 25.48 nm, respectively [49].

Au NPs were synthesized by *Stenotrophomonas maltophila* AuRed02 isolated from gold-enriched soil. Cryo-TEM observations revealed that the NPs were located on the inner cytoplasmic membrane [50].

Au NPs were also synthesized by *Hormoconis resinae* MTCC 368 isolated from soil samples collected near a refinery situated at Mathura, India. The size of the NPs observed using HR-TEM ranged from 3–20 nm. NPs extracted by centrifugation were used in the analyses [51].

Marinobacter sp. RS11 was isolated from water sampled from a solar saltern at Kakinada, India. 16 S rRNA gene sequences revealed that this bacterium resembled *Marinobacter pelagius* JCM 14804.

RS 11 was able to synthesize Au NPs. Dynamic light scattering measurements of the NPs revealed that most of the particles were smaller than 10 nm [52].

Lactobacillus kimchicus DCY51T bacterium isolated from Korean kimchi synthesized spherical Au NPs with sizes ranging from 5–30 nm. These NPs were highly stable in physiological buffer and biological media, and had an average crystallite size of 13 nm. They were better free-radical scavengers than the corresponding gold salt against 2, 2-diphenyl-1-picrylhydrazyl (DPPH) [53].

Delftia acidovorans isolated from gold nugget microbiota. In the microbiota, Au nanoparticles ranging from 10–200 nm in size were existed by *D. acidovorans*. *D. acidovorans* synthesized Au nanoparticles to protect itself from toxic soluble Au^{3+} ions. When *D. acidovorans* was grown on an agar plate in the presence of Au^{3+} ions, darkened zones developed around the colonies, indicating that *D. acidovorans* generated reducing substances [54].

Streptomyces sp. NK52 (KCTC 19739) was isolated from a laundry spot favoring alkalophiles near Pune, India. The cell-free supernatant of *Streptomyces* sp. NK52 obtained by centrifugation was used for the synthesis of the Au NPs with sizes ranging from 10–100 nm. Various shapes of NPs were observed, including triangles, rods, spheres, hexagonal prisms, rhomboids, and rectangular nanoplates [55].

Au NPs were synthesized by *Azospirillum brasilense* Sp245. The size of the NPs ranged from 5–50 nm [37].

The thermophilic bacterium *Thermus scotoductus* SA-01 also synthesized Au NPs. This bacterium is unique to South Africa and can reduce Fe(III), Mn(IV), Co(III)-EDTA, Cr(VI), and U(VI) through dissimilar pathways. Observations of ultrathin sections by TEM revealed that the Au NPs were located on the outer wall layer [56].

Au NPs were also synthesized by the cell-free filtrate of *Bacillus niabensis* 45, although details were not provided [57].

Serratia marcescens was isolated from a damp area at the Sheda Science and Technology Complex in Abuja, Nigeria. The bacterial colony was red-colored. Au NPs were synthesized by incubating the biomass or CFE of *S. marcescens* with $HAuCl_4$. Au NPs synthesis was pH-dependent: TEM observations established that smaller NPs were synthesized at lower pH [58].

Au NPs were synthesized by *Lactobacillus casei* JCM 1134 by incubating cells washed by distilled water in a $KAuCl_4$ solution. Cryo-SEM revealed that the NPs were localized outside the cell membrane. Smaller Au NPs were synthesized using the CFE [29,59].

A CFE from *Bacillus marisflavi* YCIS MN 5 isolated from estuarine water at Dabhol, India was used to synthesize Au NPs. The spherical Au NPs were catalytically active for the reduction of Congo red and methylene blue dyes. Gas chromatography-mass spectrometry of the degraded products revealed the formation of α-naphthylamine and phthalic acid from the Congo red dye and 2-methyl benzothiazole from the methylene blue dye [60].

Table 2. List of microorganisms for synthesis of Au nanoparticles and technique for confirmation of Au nanoparticles.

Metal	Microorganism	Classification	Active Molecules	Size (nm)	Techniques Used for Detection	Ref.
Au	*Verticillium* sp. AAT-TS-4	Bacteria		ca. 20	TEM, SEM, EDS, UV-vis, XRD	[7]
Au	*Rhodococcus* sp.	Bacteria		5–15	TEM, UV-vis, XRD	[35]
Au	*Escherichia coli* DH5α	Bacteria		ca. 25	TEM, SEM, UV-vis, XRD cyclic voltammograms	[42]
Au	*Rhodopseudomonas capsulata*	Bacteria	NADH	10–20	TEM, UV-vis, XRD	[43]
Au	*Shewanella algae*	Bacteria		10–20	TEM, EDS, XANES	[33, 45]
Au	*Rhodopseudomonas capsulata* (CFE)	Bacteria		10–21	TEM, EDS, UV-vis	[44]

Table 2. *Cont.*

Metal	Microorganism	Classification	Active Molecules	Size (nm)	Techniques Used for Detection	Ref.
Au	*Aspergillus niger* NCIM 616	Fungi	protein	ca. 12.8	TEM, SEM, UV-vis, XRD Zeta potential measurement	[46]
Au	*Cupriavidus metallidurans* CH34	Bacteria		100	TEM, SEM, EDS, XANES, μXRF	[47]
Au	*Rhizopus oryzae* MTCC 262	fungi		10	TEM, EDS, UV-vis, AFM	[40]
Au	*Bacillus licheniformis*	bacteria		10–100	SEM, UV-vis, XRD	[49]
Au	*Stenotrophomonas maltophilia* AuRed02	bacteria	NADPH	40	TEM, SEM, EDS, UV-vis	[50]
Au	*Hormoconis resinae* MTCC 368	Fungi		3–20	TEM, EDS, UV-vis, XRD	[51]
Au	*Marinobacter* sp. RS11	bacteria		<10	TEM, SEM, UV-vis, DLS	[52]
Au	*Lactobacillus kimchicus* DCY51	bacteria	amino acid residues surface-bound proteins	5~30	TEM,, EDS, UV-vis, XRD, DLS	[53]
Au	*Delftia acidovorans*	bacteria	Delftibactin	N.D.	TEM, UV-vis	[54]
Au	*Streptomyces* sp. NK52	bacteria		10–100	SEM, UV-vis, XRD	[55]
Au	*Azospirillum brasilense* Sp245	bacteria		5–50	TEM, UV-vis, DLS	[37]
Au	*Thermus scotoductus* SA-01	bacteria	ABC transporter	<50	TEM, EDS, UV-vis, XRD	[56]
Au	*Bacillus niabensis* 45	bacteria	cyclic peptide	N.D.	TEM, SEM, EDS, UV-vis, XRD	[57]
Au	*Serratia marcescens*	bacteria	prodigiosin	20–120	TEM, SEM, EDS, UV-vis, XRD DLS, XPS, He ion microscopy	[58]
Au	*Lactobcills casei* JCM1134	bacteria	DGDG/lactic acidlacto-N-triose	ca. 29.6	TEM, SEM, EDS, UV-vis, XRD	[29, 59]
Au	*Bacillus marisflavi* YCIS MN 5	bacteria	protein	ca. 13.5	TEM, SEM, UV-vis, XRD, DLS	[60]

2.3. Cadmium Sulfide Nanoparticles

Table 3 lists the microorganism strains used for the synthesis of CdS NPs and the techniques used for their study.

Table 3. List of microorganisms for synthesis of CdS nanoparticles and technique for confirmation of CdS nanoparticles.

Metal	Microorganism	Classification	Active Molecules	Size (nm)	Techniques Used for Detection	Ref.
CdS	*Escherichia coli* ABLE C	bacteria		2–5	TEM, EDS, STEM	[61]
CdS	*Rhodopseudomonas palustris*	bacteria	cysteine desulfhydrase	ca. 8.0	TEM, UV-vis, XRD, FT-IR, SAED	[62]
CdS	*Lactobacillus* sp	bacteria		ca. 4.9	TEM, XRD, UV-vis	[18]
CdS	*Sachharomyces cerevisae*	bacteria		ca. 3.6	TEM, XRD, UV-vis	[18]

CdS NPs were synthesized by incubating the *E. coli* strain ABLE C with $CdCl_2$ and NaS. Scanning TEM observations revealed the presence of CdS NPs in the cells. Electron diffraction patterns confirmed they had a wurtzite crystal structure [61].

CdS NPs were synthesized by incubating washed *Rhodopseudomonas palustris* cells in phosphate-buffered saline containing $CdSO_4$. SAED revealed that the NPs was polycrystalline cubic CdS. UV-vis absorption at 425 nm showed that *R. palustris* cells in the stationary phase synthesized more CdS NPs than the cells in the mid- or late-logarithmic phase [62].

Lactobacillus sp. synthesized CdS NPs. After adding solutions of $CdCl_2$ and H_2S to a dilute *Lactobacillus* sp. solution, the mixture was steam-heated. The solution was incubated at room temperature overnight. The polymorphism of the crystalline CdS NPs was investigated using XRD. Surface plasmon resonance was observed at 393 nm in the UV-vis spectrum. The estimated bandgap energy was 2.52 eV [18].

Cadmium sulfide NPs were synthesized by the yeast *Saccharomyces cerevisiae*, but the strain was not described. Cells were removed by filtration and diluted with 30% ethanol. After culturing, aqueous solutions of $CdCl_2$ and H_2S were added to the yeast solution; the combined solution was then heated at 60 °C for 10–20 min in a steam bath. The solution was cooled and incubated overnight at room temperature. Surface plasmon resonance was observed at 369 nm in the UV-vis spectrum. The estimated bandgap energy was 2.607 eV [18].

2.4. Cadmium Selenide Nanoparticles

Table 4 lists the microorganism strains used for the synthesis of CdSe NPs and the techniques used for their study.

Table 4. List of microorganisms for synthesis of CdSe nanoparticles and technique for confirmation of CdSe nanoparticles.

Metal	Microorganism	Classification	Active Molecules	Size (nm)	Techniques Used for Detection	Ref.
CdSe	*Saccharomyces cerevisiae* BY4742	fungi	NADPH	2.69–6.34	TEM, FL, laser confocal scanning microscop	[63]
CdSe	*Helminthosporum solani*	bacteria		ca. 5.5	TEM, EDS, UV-vis, FL, XPS	[64]
CdSe	*Saccharomyces cerevisiae* ATCC9763	fungi	protein	15 to 20	TEM, EDS, FL laser scanning confocal microscope	[65]
CdSe	*Pseudomonas aeruginosa* strain RB	bacteria		10/70–100	TEM, EDS	[30]
CdSe	*Fusarium oxysporum* JCM11502	fungi	superoxide dismutase	8–28	TEM, EDS, FL	[66]

Saccharomyces cerevisiae BY4742 was co-incubated with Na_2SeO, and then transported into a fresh culture with $CdCl_2$ in the dark to synthesize CdSe NPs. Additionally, in situ TEM observations revealed that the FL resulted from intracellular CdSe nanocrystals [63].

Helminthosporum solani, which is a plant pathogenic fungus, was incubated with an aqueous solution of $CdCl_2$ and $SeCl_4$ to produce CdSe NPs. The UV-vis spectrum had an absorbance band centered at 350 nm, and excitation at 380 nm resulted in an emission band centered at 430 nm in the FL spectrum, suggesting the formation of CdSe quantum dots. Monodispersed spherical NPs and a few cube-shaped particles were observed outside the cells. The EDS spectrum revealed the presence of Cd and Se, and XPS measurements suggested that the NPs were encapsulated by proteinaceous materials [64].

Saccharomyces cerevisiae ATCC9763 was also used to prepare CdSe NPs. The maximum FL intensity of bacterial solutions containing CdSe NPs was used to determine the optimal reaction condition, i.e., culturing *S. cerevisiae* with 5 mM Na_2SeO_3 for 22 h and 1 mM $CdCl_2$ for 26 h incubation. The MTT assay, which is a standard cell viability assay, and morphology observations revealed that the cytotoxicity of *S. cerevisiae* ATCC9763-prepared CdSe NPs was lower than that of thioglycolic acid (TGA)-capped CdSe and TGA-capped CdTe [65].

CdSe NPs were synthesized by *Pseudomonas aeruginosa* RB in a culture containing lactic acid as a carbon source, 1 mM selenite, and 1 mM cadmium under various conditions. The synthesis was achieved efficiently and with high purity using the reaction conditions of 25–30 °C, 0.05–10 g/L NaCl in the media, and neutral pH. Small (approximately 10 nm) and large (70–100 nm) spherical particles were observed inside and outside the cells [30].

Fusarium oxysporum JCM11502 was also used to prepare CdSe NPs. The optimal reaction conditions used solutions of 5 mM Cd(II) and Se(IV) ions at pH 7.5 and 25 °C. Ultrathin sections of *F. oxysporum* revealed that CdSe NPs were present in the intracellular space. TEM observations showed that the size of the CdSe quantum dots was less than 20 nm. These CdSe NPs were separated and purified by gel filtration chromatography, and a single sharp FL signal indicated that the NPs has a uniform size and shape [66].

2.5. Other Metal Nanoparticles

Table 5 lists the microorganism strains used for the synthesis of other metal NPs and the techniques used for their characterization.

Table 5. List of microorganisms for synthesis of various metal nanoparticles and technique for confirmation of metal nanoparticles.

Metal	Microorganism	Classification	Active Molecules	Size (nm)	Techniques Used for Detection	Ref.
Cu/CuO	*Serratia* sp.	bacteria		10–30	TEM, EDS, UV-vis, XRD, XPS	[38]
Cu	*Shewanella oneidensis*	bacteria	cytochrome	20–40	TEM, STEM, XANES EELS, SBFSEM	[67]
Gd_2O_3	*Lactobacillus* sp.	bacteria		10–20	TEM, XRD	[68]
Fe_3O_4	*Thermoanaerobacter ethanolicus* TOR-39	bacteria		41.3	TEM, XRD, zetasizer	[69]
Pb -jarosite	*Shewanella putrefaciens* CN32	bacteria		N.D.	TEM, SEM, EDS, XRD	[70]
Pb + P	*Shewanella* sp. KR-12	bacteria		3~8	TEM, EDS	[71]
PbS	*Aspergillus flavus*	fungi		35–100	TEM, EDS, UV-vis, FL, XRD	[72]
Pd	*Shewanella* sp. CNZ-1	bacteria	hydrogenase some amides	N.D.	TEM, SEM, EDS UV-vis, XRD, XPS	[73]
Pd	*Enterococcus faecalis* CCTCC M2012445	bacteria	carboxyl, hydroxyl and amine groups	N.D.	TEM, XRD, XPS, FT-IR	[74]
Pd	*Desulfovibrio vulgaris* DSM 644	bacteria		N.D.	TEM	[75]

Table 5. *Cont.*

Metal	Microorganism	Classification	Active Molecules	Size (nm)	Techniques Used for Detection	Ref.
Pt	*Desulfovibrio vulgaris* DSM 645	bacteria		N.D.	TEM	[75]
Pt	*Shewanella algae* ATCC 51181	bacteria		5	TEM, XANES	[76]
Sb_2O_3	*Lactobacillus* sp.	bacteria		3–12	TEM, XRD	[77]
Ti	*Lactobacillus* sp.	bacteria		40	TEM, XRD	[17]
TiO_2	*Lactobacillus* sp.	bacteria		ca. 24.6	TEM, XRD, SAED	[78]
TiO_2	*Sachharomyces cerevisae*	fungi		ca. 12.6	TEM, XRD, SAED	[78]
ZrO_2	*Fusarium oxysporum*	fungi		ca. 7.3	TEM, XRD	[79]

Serratia sp. was isolated from the midgut of *Stibara* sp., an insect of the Cerambycidae family of beetles found in the Northwestern Ghats of India. Cells were suspended in an aqueous solution of $CuSO_4$. XRD revealed the presence of copper oxides (CuO, Cu_2O, and Cu_4O_3) and Cu NPs [38].

Cu NPs were also synthesized by incubating a suspension of *Shewanella oneidensis* MR-1 with sodium lactate as an electron donor and $CuSO_4$ in 3-(N-morpholino)propanesulfonic acid (MOPS) buffer. Ultrathin sections observed using TEM revealed that the Cu NPs were intracellular. Furthermore, three-dimensional electron images from serial block-face SEM revealed that the NPs were dispersed across the cells. These NPs consisted of Cu(0) covered by a thin Cu_2O shell, which formed as a result of oxidation by air. The Cu_2O shell provided the particles with good catalytic activity for azide–alkyne cycloaddition and enabled a "click chemistry" reaction [67].

Lactobacillus sp. was used to synthesize near-spherical Gd_2O_3 NPs. Gadolinium acetate was used as the source of Gd ions. The SAED pattern and XRD spectrum established the crystal structure of the Gd_2O_3 [68].

Fe_3O_4 NPs were synthesized using *Thermoanaerobacter ethanolicus* TOR-39. This thermophilic bacterial strain was incubated with glucose as an electron donor, MOPS as a pH buffer, and amorphous Fe(III) oxyhydroxide as an electron acceptor. A superconducting quantum interference magnetometer revealed that the Fe_3O_4 NPs had higher coercivity and less remanence than those made using chemical methods [69].

Shewanella putrefaciens CN32 is a subsurface chemoautotrophic anaerobe capable of using Fe(III) during dissimilatory iron reduction. The NPs containing Pb and P detected by EDS were synthesized in a suspension of the CN32 cells with the mineral plumbojarosite ($PbFe_6(SO_4)_4(OH)_{12}$) [70].

Lead was accumulated by *Shewanella* sp. KR-12 isolated from river sediment in northeast Taiwan. Notably, amorphous Pb NPs were synthesized when incubated with $Pb(NO)_3$. Spherical particles ranged from 3–8 nm in size. while those on pilus-like structures emerging from bacteria ranged from 2–4 nm. The NPs formed in linear or curved patterns within the bacteria; EDS spectra revealed that the linear localization contained elemental Pb and P [71].

Aspergillus flavus, an endophytic fungus isolated from a medicinal plant *Nothapodytes foetida*, tolerates lead and sulfide. PbS NPs were synthesized by incubating *A. flavus* in culture media containing lead acetate and sodium sulfide. The peak centered at 300 nm in the UV-vis spectrum, which is consistent with PbS NPs. The optical bandgap of the PbS NPs was 3.08 eV, which is markedly higher than that of the bulk PbS (0.41 eV). The absorbance properties of the PbS NPs enabled their use for the detection of As(III) ion [72].

Pd NPs were synthesized by *Shewanella* sp. CNZ-1, which is an electrochemically active bacterium isolated from marine sediments. Pd NPs were synthesized on the surface of CNZ-1 cells by adding Na_2PdCl_4 and sodium lactate as an electron donor to a CNZ-1 solution. The Pd NPs catalyzed reduction of 4-nitrophenol by $NaBH_4$. The *Shewanella oneidensis* MR-1 strain was also able to synthesize Pd NPs,

but the Pd NPs synthesized by CNZ-1 were more effective than those prepared by MR-1 in mediating 4-nitrophenol reduction [73].

Pd NPs were also synthesized by incubating *Enterococcus faecalis* CCTCC M2012445 suspension in MOPS buffer with Na_2PdCl_4 and sodium formate as electron donor. XRD analysis revealed Pd NPs synthesis. According to TEM observation of the cell, Pd NPs were located at the cell membrane and inside the cell [74].

Desulfovibrio vulgaris DSM 644 synthesized Pt NPs and Pd NPs by incubating in MOPS buffer with Na_2PdCl_4 or $PtCl_4$. TEM observation showed that both NPs were located on the surface and in the periplasmic space. Pt NPs synthesized by *D. vulgaris* had a high catalytic activity in pharmaceutical products removal. As pharmaceutical products are thought as one of the most alarming emergent pollutants, these Pt NPs was expected as excellent catalyst [75].

Pt NPs were synthesized by incubating *Shewanella algae* ATCC 51181 in bicarbonate buffer with H_2PtCl_6 solution and sodium lactate as electron donor under anaerobic conditions. These NPs were synthesized within 60 min. Furthermore, these NPs were located in the periplasm. XANES spectrum of PtNPs synthesized bv *S. algae* was identical to the Pt(0), not Pt(IV) and Pt(II) [76].

Antimony chloride solution was added to *Lactobacillus* sp. from pharmaceutical-grade lactic acid bacillus spore tablets (SporeLac DS; Sanyko Pharmaceuticals, Japan), and the mixed solution was heated in a steam bath at 80 °C for 5–10 min. The XRD pattern of the product was consistent with n-Sb_2O_3. Williamson–Hall plots of the XRD data indicated low lattice strain. Individual Sb_2O_3 NPs and a few aggregates were observed using TEM [77].

Adding a TiO_2 solution to a culture solution of *Lactobacillus* strain generated Ti NPs. Scherrer's equation was used to estimate the average particle size from the XRD pattern [17].

TiO_2 NPs were synthesized by *Lactobacillus* sp. obtained from buttermilk. A mixture of dilute culture and $TiO(OH)_2$ solution was heated on a steam bath to 60 °C and held for 10–20 min. After cooling, the solution was incubated at room temperature for 12–48 h. Electron diffraction and XRD measurements established that the NPs were n-TiO_2 [78].

Saccharomyces cerevisiae (strain not specified) also synthesized TiO_2 NPs. NPs formed when a $TiO(OH)_2$ solution was added to an ethanoic *S. cerevisiae* solution. Electron diffraction and XRD measurements confirmed that the NPs were n-TiO_2 [78].

ZrO_2 NPs were synthesized by incubating *Fusarium oxysporum* in a solution of K_2ZrF_6. XRD measurements revealed that the ZrO_2 NPs consisted of a mixture of monoclinic and tetragonal phases [79].

3. Active Molecules in Metal Nanoparticle Synthesis by Microorganisms

Extracellular polymeric substances (EPS) of *E. coli* K12 Ag NPs were synthesized by adding $AgNO_3$ to a culture solution. Comparing the Fourier transform-infrared (FT-IR) and ^{13}C nuclear magnetic resonance (NMR) spectra of the EPS before and after reaction with Ag^+ revealed that the hemiacetal groups of the sugars in the EPS contributed to Ag NPs synthesis (Figure 5). The antibacterial activity of Ag^+ ions was mitigated because the synthesized Ag NPs in the EPS were not inside cells [36].
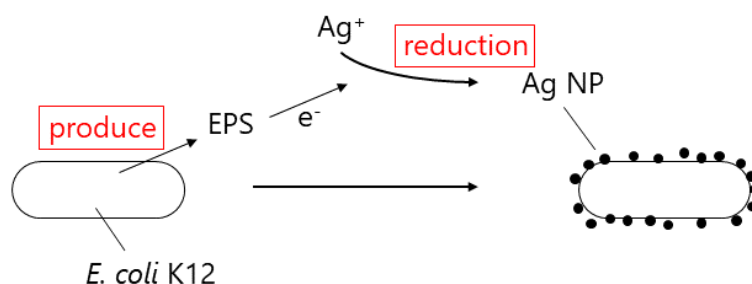

Figure 5. The mechanism of Ag NPs synthesis by *E. coli* K12. Extracellular polymeric substances (EPS) produced by the cell reduced Ag ion and synthesized Ag NPs.

The synthesis of Ag NPs affected the monosaccharide composition of capsular exopolysaccharides from
Lactobacillus strains. This result suggests that different *Lactobacillus* strain synthesized different NPs or did not synthesize Ag NPs [40].

The FT-IR spectrum of Au NPs synthesized by the culture supernatant from *A. niger* NCIM 616 indicated the presence of amide linkages. This result suggested that some protein contributed to the synthesis and stabilization of the NPs [46].

The FT-IR spectrum of Au NPs synthesized by *S. maltophilia* AuRed02 suggests that NPs were capped with negatively charged phosphate groups from NADP. To reveal the synthesis mechanism, the CFE and the CFE with NADPH were separately mixed with Au^{3+}. The Au NPs were synthesized only by the mixture of CFE and NADPH, indicating that an NADPH-dependent reductase enzyme in CFE reduced Au^{3+} to Au(0) [50].

Delftibactin, a gold-interacting nonribosomal peptide purified from *D. acidovorans*, was crucial to Au NPs synthesis by this bacterium. Mixing delftibactin and $AuCl_3$ rapidly (within seconds) induced the synthesis of Au NPs and octahedral gold platelets at room temperature and neutral pH. Additionally, delftibactin protected the cell from toxic soluble gold [54].

In the Au NPs synthesis by *A. brasilencse*, extracellular phenol-oxidizing enzymes (laccases and Mn peroxidases) acted as reducing agents [37].

Cell-free extracts from *T. scotoductus* SA-01 were size-fractionated by an Amicon® stirred cell fitted with a UF 30 MWCO membrane (Osmonics Inc.). Au NPs were synthesized by incubation of soluble proteins (> 30 kDa) with $HAuCl_4$. Analysis of the N-terminal sequence revealed that the protein synthesizing the Au NPs was a peptide-binding protein ABC transporter. The cysteine–disulfide bridge electron shuttle mechanism of the ABC transporter seemed to be involved in the Au NPs synthesis [56].

To identify the active molecules for Au NPs synthesis by *B. niabensis* 45, the crude peptide was analyzed by preparative high-performance liquid chromatography. Only the material corresponding to one peak was effective at synthesizing Au NPs. The results of matrix-assisted laser desorption/ionization-time of-flight mass spectrometry (MALDI-TOF-MS), electrospray ionization mass spectrometry (ESI-MS), and thin-layer chromatography (TLC) assay established that a cyclic peptide was the active agent. The cyclic peptide formed face-centered-cubic NPs with sizes ranging from 10–20 nm and formed an antibiofilm against *P. aeruginosa* PAO1 and *S. aureus* ATCC 25923 with low or no toxicity [57].

Prodigiosin was the active molecule in the synthesis of Au NPs by *S. marcescens*. Prodigiosin is a tripyrrole red pigment and a secondary metabolite by *S. marcescens*. Helium ion microscopy established that prodigiosin capped the Au NPs [58].

In the Au NPs synthesis by *L. casei* JCM 1134, glycolipids in the cell membrane and extracellular components were key molecules. Comparison of the *L. casei* components before and after addition of a $K(AuCl_4)$ solution revealed significantly lower unsaturated lipids level after the addition. The NMR and mass spectra revealed that diglycosyldiacylglycerol (DGDG) and triglycosyldiacylglycerol (TGDG) bearing unsaturated fatty acids were more reduced after the formation of the Au NPs. Au NPs were synthesized by DGDG purified from JCM 1134 in vitro [29]. Furthermore, the NMR and MS spectra of purified extracellular components revealed that lacto-*N*-triose and lactic acid induced the synthesis of Au NPs. Smaller NPs were synthesized by the extracellular components, indicating that these components contributed to dispersion of the particles (Figure 6) [59]

FT-IR spectrum of CFE of *B. marisflavi* YCIS MN 5 showed that protein existed in the CFE and the protein contributed in Au NPs synthesis. In addition, comparing FT-IR spectrum of the CFE and Au NPs synthesized by the CFE showed that the NPs were masked by the protein in CFE (Figure 7) [60].
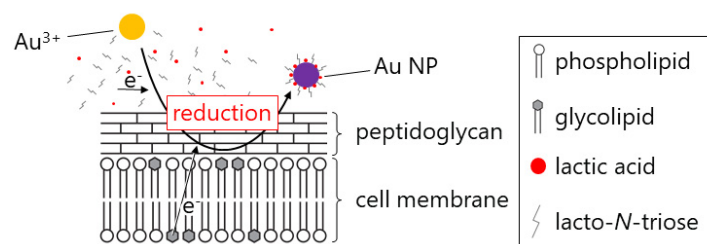
Figure 6. The mechanism of Au NPs synthesis by *L. casei*. Au ion was reduced by diglycosyldiacylglycerol (DGDG) (glycolipid in cell membrane) and lacto-*N*-triose. Au crystals were kept small by lactic acid secreted from the cell.
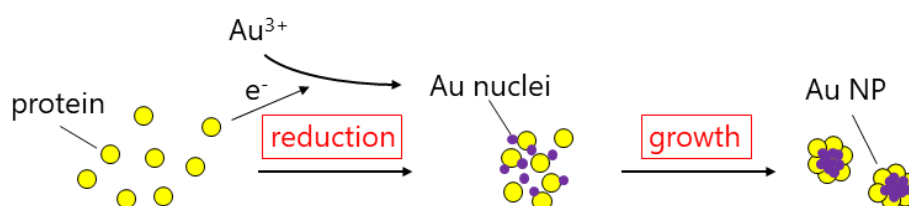

Figure 7. The mechanism of Au NPs synthesis by CFE of *B. marisflavi* YCIS MN 5. Protein in the CFE reduced Au ion and produced Au nuclei. The Au nuclei would grow to Au NP.

In the synthesis of CdSe NPs by *S, cerevisiae* ATCC9763, capping of the NPs with intracellular protein molecules improved dispersion in water. The presence of protein ensured that the biosynthesized NPs had much lower cytotoxicity compared with hydrothermally synthesized TGA-capped CdSe [65].

Mycelial cells were examined before and after treatment of *F. oxysporum* with a mixed solution of Cd(II) and Se(IV) ions to reveal the molecular dynamics of CdSe NPs synthesis. Sodium dodecyl sulfate–polyacrylamide gel electrophoresis (SDS-PAGE) established that the amount of superoxide dismutase decreased, and FL microscopy revealed that the amount of cytoplasmic superoxide increased, during the CdSe NPs synthesis. These results indicate that superoxide contributed to CdSe NPs synthesis [66].

Pd NPs were prepared by mixing a solution of live *Shewanella* sp. CNZ-1 cells and sodium lactate with a Pd(II) solution. Hot-killed CNZ-1 cells could not induce NPs synthesis. One or more hydrogenases were likely involved in the Pd(II) reduction by CNZ-1 in the presence of sodium lactate as an electron donor, because autoclaved bacterial cells exhibited no hydrogenase activity (Figure 8). Additionally, the FT-IR spectrum of the Pd NPs was consistent with the interaction of some amides with the Pd NPs [73].
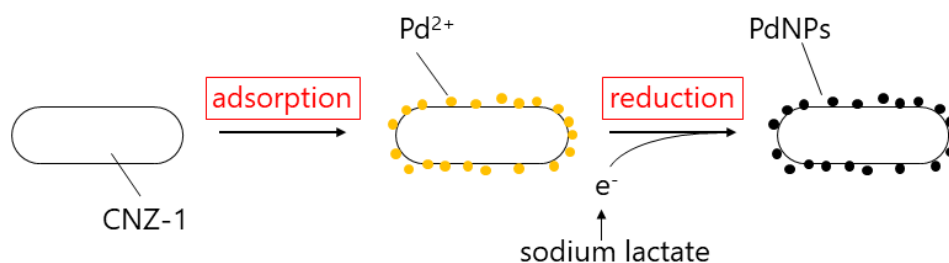

Figure 8. The mechanism of Pd NPs synthesis by *Shewanella* sp. CNZ-1. At first, the bacteria adsorbed Pd ion. The Pd ion were reduced by electron from added sodium lactate.

Although Pd NPs were synthesized by incubating *E. faecalis* Pd solution with sodium formate, Pd was not reduced without sodium formate. This result indicated that the *E. faecalis* cells provided a wide and uniform place for Pd NPs crystallization. The surface character of *E. faecalis* was revealed by XPS and FT-IR spectrum. These results showed that chemicals with carboxyl groups, hydroxyl groups, and amine groups participated in Pd recovery (Figure 9) [74].
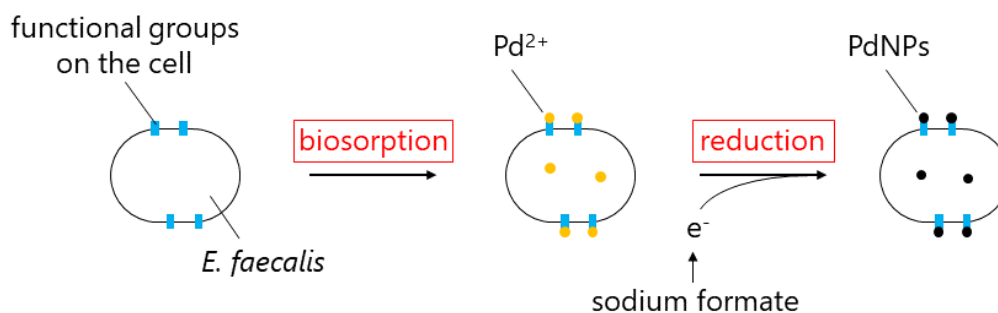
Figure 9. The mechanism of Pd NPs synthesis by *E. faecalis*. At first, the Pd ion was adsorbed on the cell and uptake into the cell. Carboxyl groups, hydroxyl groups, and amine groups were participated in adsorption. Next, the Pd ion was reduced. The ion donor was sodium formate.

F. oxysporum hydrolyzed ZrF_6^{2-} ions to form ZrO_2 NPs. Native and SDS-PAGE of the extracellular protein in the absence and presence of aqueous ZrF_6^{2-} ions revealed the disappearance of proteins with molecular weights of about 24 and 28 kDa. The proteins were loaded onto a cation exchange matrix to determine the nature of the charge on the proteins. The eluted fractions hydrolyzed ZrF_6^{2-}, indicating that cationic proteins were involved in the ZrO_2 NPs synthesis [79].

In addition, several publications have focused on the synthesis of metal NPs using genetically modified *E. coli*.

Au-Pd core-shell NPs were synthesized by AtPCS1-*E. coli*. The AtPCS1-*E. coli* was incubated in $HAuCl_4$ solution, and then in K_2PdCl_4 solution. Their catalytic behavior was investigated using two methods: Chemiluminescence (CL) and benzyl alcohol oxidation (BAO). In the former, the CL of the mixture of Au-Pd NPs extracted by ultrasonication, luminol, and H_2O_2 was measured. In the BAO test, a mixture of H_2O_2, cetrimonium bromide, and Au-Pd NPs generated benzyl alcohol, benzaldehyde, and benzoic acid, which was detected using gas chromatography and mass spectrometry. These tests demonstrated that the Au-Pd NPs were catalytically active [80].

The cysteine desulfhydrase gene of *Treponema denticola* was over-expressed in *E. coli* to synthesize CdS NPs. Incubation of the cells in a culture medium supplemented with cadmium ions and cysteine resulted in CdS NPs forming on the cell wall [81].

Additionally, CdS NPs were biosynthesized via *Arabidopsis thaliana* phytochelatin synthase-modified *E. coli* (CdS/AtPCS1-*E. coli*). Biosynthesis of CdS NPs was greatly enhanced through expression of the AtPCS1 gene inside the *E. coli* cells by the pET28b vector due to the generation of phytochelatins (PCs; (γ-Glu-Cys)n-Gly, n ≥ 2), which efficiently captured Cd^{2+} ions [82].

Tables 1–6 list the active molecules used for the synthesis of metal NPs in microorganisms.

Table 6. List of genetically modified bacteria for synthesis of metal nanoparticles and technique for confirmation of metal nanoparticles.

Metal	Microorganism	Classification	Active Molecules	Size (nm)	Techniques Used for Detection	Ref.
Au-Pd	*Escherichia coli*	bacteria	AtPCS1	ca. 32.3	TEM, SEM, UV-vis, XRD	[80]
CdS	*Escherichia coli*	bacteria	cysteine desulfhydrase	<50	TEM, EDS	[81]
CdS	*Escherichia coli*	bacteria	AtPCS1	35.8	TEM, EDS, UV-vis, FL	[82]

4. Purification of NPs Synthesized by Microorganisms

A few reports have mentioned the potential applications of NPs synthesized by microorganisms. As many organic molecules from the cell components are present in the NPs solution synthesized by microorganisms, purification and isolation NPs from such contaminants are necessary for application.

Ag NPs synthesized by *E. coli* were isolated by washing, dialysis, and ultracentrifugation. At first, the Ag NPs were centrifuged and resuspended by water in order to eliminate remaining Ag ion. Next, the suspension was subjected to a dialysis tube and cutoff 12,000 molecular weight. Finally, the NPs were suspended in HEPES buffer and subjected to ultracentrifugation [83].

The supernatant of Ag NPs solution synthesized by CFE of *Bacillus* sp. AZ1 was air dried to obtain Ag NPs. The treatment of air drying broke the cell membrane to reduce the toxicity of bacterial cells. These separated Ag NPs had antimicrobial activity for the Gram-negative (*E. coli* and *Salmonella typhi*) and Gram-positive (*Staphylococcus epidermis*, and *Staphylococcus aureus*) bacteria. Especially, these NPs had high antimicrobial activity for *E. coli* [75].

Pt NPs synthesized by *D. vulgaris* were purified by centrifugation with water and acetone to wash and drying at room temperature overnight. These purified NPs were used as catalysis for removal of pharmaceutical products (ciprofloxacin, sulfamethoxazole, ibuprofen, and 17β-estradiol). In the result, these Pt NPs had high catalytic activities to remove ciprofloxacin, sulfamethoxazole, and 17β-estradiol [84].

However, negative effects might occur by separation technique. For example, the solution color of Ag NPs synthesized by *L. casei* were degraded by both filtrating and centrifuging. This result suggested that Ag NPs were aggregated or entrapped in the biomass [73].

On the other hand, there are the report that assembly of bacteria and NPs promote synergy effects. The particle-bacterium assembly facilitated direct electron transfer between proteins and an electrode by immobilizing hemoglobin [42].

5. Conclusions

Herein, we have reviewed the synthesis of metal NPs by microorganisms. Over the last half-century, various metal NPs have been synthesized by numerous microorganisms. In some studies, the active substances for their synthesis were identified from microorganism extracts. In general, the smaller size of metal NPs shows the greater catalytic activities [14]. Genetically modified microorganisms can control the localization and amounts of activity molecules inside or outside the cell. Such genetically control methods can regulate the size and shape of metal NPs. As many biological molecules exist in the microorganism suspension, it is difficult to isolate metal NPs. However, analyses of molecular mechanisms can reveal the active molecules binding to the surface of metal NPs. If these active molecules may be useful for the applications such as biocompatibility, biomarker, and anti-cancer effects, we can use these metal NPs as high functional organic–inorganic hybrid materials.

As shown in this review, there are many reports of easy synthesis of various metal NPs by microorganisms. In addition, metal NPs synthesized by microorganisms were reported as more stable and low toxicity. Ag NPs synthesized by *Staphylococcus aureus* were less toxicity than chemically synthesized Ag NPs [81]. These metal NPs are biocompatible and may be useful in medical field.

Author Contributions: Conceptualization, Y.K. and M.S.; writing—original draft preparation, Y.K. and M.S.; writing—review and editing, Y.K. and M.S.; supervision, M.S.; funding acquisition, Y.K. and M.S. All authors have read and agreed to the published version of the manuscript.

Conflicts of Interest: The authors declare no conflict of interest.

References

1. Gahlawat, G.; Shikha, S.; Chaddha, B.S.; Chaudhuri, S.R.; Mayilraj, S.; Choudhury, A.R. Microbial glycolipoprotein-capped silver nanoparticles as emerging antibacterial agents against cholera. *Microb. Cell Factories* **2016**, *15*, 25. [CrossRef]
2. Kaur, A.; Gupta, U. A review on applications of nanoparticles for the preconcentration of environmental pollutants. *J. Mater. Chem.* **2009**, *19*, 8279. [CrossRef]

3. Li, X.; Xu, H.; Chen, Z.; Chen, G. Biosynthesis of Nanoparticles by Microorganisms and Their Applications. *J. Nanomater.* **2011**, *2011*, 1–16. [CrossRef]

4. Lohse, S.E.; Murphy, C.J. Applications of colloidal inorganic nanoparticles: From medicine to energy. *J. Am. Chem. Soc.* **2012**, *134*, 15607–15620. [CrossRef]

5. Chao, J.; Liu, J.; Yu, S.; Feng, Y.; Tan, Z.; Liu, R.; Yin, Y. Speciation Analysis of Silver Nanoparticles and Silver Ions in Antibacterial Products and Environmental Waters via Cloud Point Extraction-Based Separation. *Anal. Chem.* **2011**, *83*, 6875–6882. [CrossRef]

6. Storhoff, J.J.; Lazarides, A.A.; Mucic, R.C.; Mirkin, C.A.; Letsinger, R.L.; Schatz, G.C. What Controls the Optical Properties of DNA-Linked Gold Nanoparticle Assemblies? *J. Am. Chem. Soc.* **2000**, *122*, 4640–4650. [CrossRef]

7. Deplanche, K.; Bennett, J.A.; Mikheenko, I.P.; Omajali, J.; Wells, A.S.; Meadows, R.E.; Wood, J.; Macaskie, L.E. Catalytic activity of biomass-supported Pd nanoparticles: Influence of the biological component in catalytic efficacy and potential application in 'green' synthesis of fine chemicals and pharmaceuticals. *Appl. Catal. B Environ.* **2014**, *147*, 651–665. [CrossRef]

8. Jukk, K.; Kongi, N.; Matisen, L.; Kallio, T.; Kontturi, K.; Tammeveski, K. Electroreduction of oxygen on palladium nanoparticles supported on nitrogen-doped graphene nanosheets. *Electrochim. Acta* **2014**, *137*, 206–212. [CrossRef]

9. Safavi, A.; Maleki, N.; Farjami, F.; Farjami, E. Electrocatalytic oxidation of formaldehyde on palladium nanoparticles electrodeposited on carbon ionic liquid composite electrode. *J. Electroanal. Chem.* **2009**, *626*, 75–79. [CrossRef]

10. García-Domínguez, P.; Nevado, C. Au–Pd bimetallic catalysis: The importance of anionic ligands in catalyst speciation. *J. Am. Chem. Soc.* **2016**, *138*, 3266–3269. [CrossRef]

11. Xu, J.; White, T.; Li, P.; He, C.; Yu, J.; Yuan, W.; Han, Y. Biphasic Pd−Au alloy catalyst for low-temperature CO oxidation. *J. Am. Chem. Soc.* **2010**, *132*, 10398–10406. [CrossRef]

12. Cheong, S.; Graham, L.; Brett, G.L.; Henning, A.M.; Watt, J.; Miedziak, P.J.; Song, M.; Takeda, Y.; Taylor, S.H.; Tilley, R.D. Au–Pd core–Shell nanoparticles as alcohol oxidation catalysts: Effect of shape and composition. *ChemSusChem* **2013**, *6*, 1858–1862. [CrossRef]

13. Su, R.; Tiruvalam, R.; He, Q.; Dimitratos, N.; Kesavan, L.; Hammond, C.; Lopez-Sanchez, J.A.; Bechstein, R.; Kiely, C.J.; Hutchings, G.J. Promotion of phenol photodecomposition over TiO$_2$ using Au, Pd, and Au–Pd nanoparticles. *ACS Nano* **2012**, *6*, 6284–6292. [CrossRef] [PubMed]

14. Hamasaki, T.; Kashiwagi, T.; Imada, T.; Nakamichi, N.; Aramaki, S.; Toh, K.; Morisawa, S.; Shimakoshi, H.; Hisaeda, Y.; Shirahata, S. Kinetic Analysis of Superoxide Anion Radical-Scavenging and Hydroxyl Radical-Scavenging Activities of Platinum Nanoparticles. *Langmuir* **2008**, *24*, 7354–7364. [CrossRef]

15. Jin, T.; Yan, M.; Yamamoto, Y. Click Chemistry of Alkyne–Azide Cycloaddition using Nanostructured Copper Catalysts. *ChemCatChem* **2012**, *4*, 1217–1229. [CrossRef]

16. Kessler, R. Engineered Nanoparticles in Consumer Products: Understanding a New Ingredient. *Environ. Health Perspect.* **2011**, *119*, A120–A125. [CrossRef]

17. Prasad, K.; Jha, A.; Kulkarni, A. Lactobacillus assisted synthesis of titanium nanoparticles. *Nanoscale Res. Lett.* **2007**, *2*, 248–250. [CrossRef]

18. Prasad, K.; Jha, A.K. Biosynthesis of CdS nanoparticles: An improved green and rapid procedure. *J. Colloid Interface Sci.* **2010**, *342*, 68–72. [CrossRef] [PubMed]

19. Compeán-Jasso, M.E.; Ruiz, F.; Martínez, J.R.; Herrera-Gómez, A. Magnetic properties of magnetite nanoparticles synthesized by forced hydrolysis. *Mater. Lett.* **2008**, *62*, 4248–4250. [CrossRef]

20. Kim, H.; Kang, Y.; Park, H.; Lee, K.; Yang, S.; Jung, H.; Seo, D. Effects of the dispersion of zirconium dioxide nanoparticles on high performance electro-optic properties in liquid crystal devices. *Liquid Cryst.* **2011**, *38*, 871–875. [CrossRef]

21. Trindade, T.; O'Brien, P.; Pickett, N.L. Nanocrystalline Semiconductors: Synthesis, Properties, and Perspectives. *Chem. Mater.* **2001**, *13*, 3843–3858. [CrossRef]

22. Faraon, A.; Englund, D.; Fushman, I.; Vučković, J.; Stoltz, N.; Petroff, P. Local quantum dot tuning on photonic crystal chips. *Appl. Phys. Lett.* **2007**, *90*, 213110. [CrossRef]

23. Muthalif, M.P.A.; Sunesh, C.D.; Choe, Y. Enhanced light absorption and charge recombination control in quantum dot sensitized solar cells using tin doped cadmium sulfide quantum dots. *J. Colloid Interface Sci.* **2019**, *534*, 291–300. [CrossRef] [PubMed]

24. Wang, D.; Li, X.; Zheng, L.; Qin, L.; Li, S.; Ye, P.; Li, Y.; Zou, J. Size-controlled synthesis of CdS nanoparticles confined on covalent triazine-based frameworks for durable photocatalytic hydrogen evolution under visible light. *Nanoscale* **2018**, *10*, 19509–19516. [CrossRef] [PubMed]

25. Frens, G. Controlled Nucleation for the Regulation of the Particle Size in Monodisperse Gold Suspensions. *Nat. Phys. Sci.* **1973**, *241*, 20–22. [CrossRef]

26. Murray, C.; Norris, D.J.; Bawendi, M.G. Synthesis and characterization of nearly monodisperse CdE (E = sulfur, selenium, tellurium) semiconductor nanocrystallites. *J. Am. Chem. Soc.* **1993**, *115*, 8706–8715. [CrossRef]

27. Blakemore, R. Magnetotactic bacteria. *Science* **1975**, *190*, 377–379. [CrossRef]

28. Korbekandi, H.; Iravani, S.; Abbasi, S. Optimization of biological synthesis of silver nanoparticles using *Lactobacillus casei* subsp. casei. *J. Chem. Technol. Biotechnol.* **2012**, *87*, 932–937. [CrossRef]

29. Kikuchi, F.; Kato, Y.; Furihata, K.; Kogure, T.; Imura, Y.; Yoshimura, E.; Suzuki, M. Formation of gold nanoparticles by glycolipids of *Lactobacillus casei*. *Sci. Rep.* **2016**, *6*, 34626. [CrossRef]

30. Ayano, H.; Kuroda, M.; Soda, S.; Ike, M. Effects of culture conditions of Pseudomonas aeruginosa strain RB on the synthesis of CdSe nanoparticles. *J. Biosci. Bioeng.* **2015**, *119*, 440–445. [CrossRef]

31. Bruins, M.R.; Kapil, S.; Oehme, F.W. Microbial resistance to metals in the environment. *Ecotoxicol. Environ. Saf.* **2000**, *45*, 198–207. [CrossRef] [PubMed]

32. Park, J.H.; Lamb, D.; Paneerselvam, P.; Choppala, G.; Bolan, N.; Chung, J. Role of organic amendments on enhanced bioremediation of heavy metal (loid) contaminated soils. *J. Hazard. Mater.* **2011**, *185*, 549–574. [CrossRef]

33. Konishi, Y.; Tsukiyama, T.; Ohno, K.; Saitoh, N.; Nomura, T.; Nagamine, S. Intracellular recovery of gold by microbial reduction of $AuCl_4^-$ ions using the anaerobic bacterium *Shewanella algae*. *Hydrometallurgy* **2006**, *81*, 24–29. [CrossRef]

34. Joerger, R.; Klaus, T.; Granqvist, C.G. Biologically Produced Silver–Carbon Composite Materials for Optically Functional Thin-Film Coatings. *Adv. Mater.* **2000**, *12*, 407–409. [CrossRef]

35. Ahmad, A.; Senapati, S.; Khan, M.I.; Kumar, R.; Ramani, R.; Srinivas, V.; Sastry, M. Intracellular synthesis of gold nanoparticles by a novel alkalotolerant actinomycete, *Rhodococcus* species. *Nanotechnology* **2003**, *14*, 824. [CrossRef]

36. Kang, F.; Alvarez, P.J.; Zhu, D. Microbial Extracellular Polymeric Substances Reduce Ag+ to Silver Nanoparticles and Antagonize Bactericidal Activity. *Environ. Sci. Technol.* **2014**, *48*, 316–322. [CrossRef] [PubMed]

37. Kupryashina, M.; Vetchinkina, E.; Burov, A.; Ponomareva, E.; Nikitina, V. Biosynthesis of gold nanoparticles by *Azospirillum brasilense*. *Microbiology* **2013**, *82*, 833–840. [CrossRef]

38. Hasan, S.; Singh, S.; Parikh, R.Y.; Dharne, M.S.; Patole, M.S.; Prasad, B.L.V.; Shouche, Y.S. Bacterial Synthesis of Copper/Copper Oxide Nanoparticles. *J. Nanosci. Nanotechnol.* **2008**, *8*, 3191–3196. [CrossRef]

39. Ahmad, A.; Mukherjee, P.; Senapati, S.; Mandal, D.; Khan, M.I.; Kumar, R.; Sastry, M. Extracellular biosynthesis of silver nanoparticles using the fungus *Fusarium oxysporum*. *Colloids Surf. B Biointerfaces* **2003**, *28*, 313–318. [CrossRef]

40. Garmasheva, I.; Kovalenko, N.; Voychuk, S.; Ostapchuk, A.; Livins'ka, O.; Oleschenko, L. Lactobacillus species mediated synthesis of silver nanoparticles and their antibacterial activity against opportunistic pathogens in vitro. *BioImpacts BI* **2016**, *6*, 219–223. [CrossRef]

41. Sani, N.J.; Aminu, B.M.; Mukhtar, M.D. Eco-friendly synthesis of silver nanoparticles using *Lactobacillus delbrueckii* subsp. bulgaricus isolated from kindrimo (locally fermented milk) in Kano State, Nigeria. *Bayero J. Pure Appl. Sci.* **2018**, *10*, 481. [CrossRef]

42. Du, L.; Jiang, H.; Liu, X.; Wang, E. Biosynthesis of gold nanoparticles assisted by Escherichia coli DH5α and its application on direct electrochemistry of hemoglobin. *Electrochem. Commun.* **2007**, *9*, 1165–1170. [CrossRef]

43. He, S.; Guo, Z.; Zhang, Y.; Zhang, S.; Wang, J.; Gu, N. Biosynthesis of gold nanoparticles using the bacteria *Rhodopseudomonas capsulata*. *Mater. Lett.* **2007**, *61*, 3984–3987. [CrossRef]

44. He, S.; Zhang, Y.; Guo, Z.; Gu, N. Biological Synthesis of Gold Nanowires Using Extract of *Rhodopseudomonas capsulata*. *Biotechnol. Prog.* **2008**, *24*, 476–480. [CrossRef]

45. Konishi, Y.; Tsukiyama, T.; Tachimi, T.; Saitoh, N.; Nomura, T.; Nagamine, S. Microbial deposition of gold nanoparticles by the metal-reducing bacterium *Shewanella algae*. *Electrochim. Acta* **2007**, *53*, 186–192. [CrossRef]

46. Bhambure, R.; Bule, M.; Shaligram, N.; Kamat, M.; Singhal, R. Extracellular Biosynthesis of Gold Nanoparticles using Aspergillus niger—Its Characterization and Stability. *Chem. Eng. Technol.* **2009**, *32*, 1036–1041. [CrossRef]

47. Reith, F.; Etschmann, B.; Grosse, C.; Moors, H.; Benotmane, M.; Monsieurs, P.; Grass, G.; Doonan, C.; Vogt, S.; Lai, B.; et al. Mechanisms of gold biomineralization in the bacterium *Cupriavidus metallidurans*. *Proc. Natl. Acad. Sci. USA* **2009**, *106*, 17757. [CrossRef]

48. Das, S.K.; Das, A.R.; Guha, A.K. Gold Nanoparticles: Microbial Synthesis and Application in Water Hygiene Management. *Langmuir* **2009**, *25*, 8192–8199. [CrossRef]

49. Kalishwaralal, K.; Deepak, V.; Ram Kumar Pandian, S.; Gurunathan, S. Biological synthesis of gold nanocubes from *Bacillus licheniformis*. *Bioresour. Technol.* **2009**, *100*, 5356–5358. [CrossRef]

50. Nangia, Y.; Wangoo, N.; Goyal, N.; Shekhawat, G.; Suri, C.R. A novel bacterial isolate *Stenotrophomonas maltophilia* as living factory for synthesis of gold nanoparticles. *Microb. Cell Factories* **2009**, *8*, 39. [CrossRef]

51. Mishra, A.; Bhadauria, S.; Gaur, M.; Pasricha, R. Extracellular microbial synthesis of gold nanoparticles using fungus *Hormoconis resinae*. *JOM* **2010**, *62*, 45–48. [CrossRef]

52. Sharma, N.; Pinnaka, A.K.; Raje, M.; Fnu, A.; Bhattacharyya, M.S.; Choudhury, A.R. Exploitation of marine bacteria for production of gold nanoparticles. *Microb. Cell Factories* **2012**, *11*, 86. [CrossRef]

53. Markus, J.; Mathiyalagan, R.; Kim, Y.; Abbai, R.; Singh, P.; Ahn, S.; Perez, Z.E.J.; Hurh, J.; Yang, D.C. Intracellular synthesis of gold nanoparticles with antioxidant activity by probiotic *Lactobacillus kimchicus* DCY51T isolated from Korean kimchi. *Enzym. Microb. Technol.* **2016**, *95*, 85–93. [CrossRef]

54. Johnston, C.W.; Wyatt, M.A.; Li, X.; Ibrahim, A.; Shuster, J.; Southam, G.; Magarvey, N.A. Gold biomineralization by a metallophore from a gold-associated microbe. *Nat. Chem. Biol.* **2013**, *9*, 241–243. [CrossRef] [PubMed]

55. Prakash, D.; Mahale, V.; Bankar, A.; Nawani, N.; Mahale, V. Biosynthesis of colloidal gold nanoparticles by *Streptomyces* sp. NK52 and its anti-lipid peroxidation activity. *Indian J. Exp. Biol.* **2013**, *51*, 969.

56. Erasmus, M.; Cason, E.; Cason, E.; van Marwijk, J.; van Marwijk, J.; Botes, E.; Botes, E.; Gericke, M.; Gericke, M.; van Heerden, E.; et al. Gold nanoparticle synthesis using the thermophilic bacterium *Thermus scotoductus* SA-01 and the purification and characterization of its unusual gold reducing protein. *Gold Bull.* **2014**, *47*, 245–253. [CrossRef]

57. Li, Y.; Li, Y.; Li, Q.; Fan, X.; Gao, J.; Luo, Y. Rapid Biosynthesis of Gold Nanoparticles by the Extracellular Secretion of *Bacillus niabensis* 45: Characterization and Antibiofilm Activity. *J. Chem.* **2016**, *2016*, 1–7. [CrossRef]

58. Dozie-Nwachukwu, S.; Obayemi, J.; Danyuo, Y.; Etuk-Udo, G.; Chi, Y.; Hu, J.; Anuku, N.; Odusanya, O.; Malatesta, K.; Soboyejo, W. Biosynthesis of Gold Nanoparticles and Gold/Prodigiosin Nanoparticles with *Serratia marcescens* Bacteria. *Waste Biomass Valor* **2017**, *8*, 2045–2059. [CrossRef]

59. Kato, Y.; Yoshimura, E.; Suzuki, M. Synthesis of Gold Nanoparticles by Extracellular Components of *Lactobacillus casei*. *ChemistrySelect* **2019**, *4*, 7331–7337. [CrossRef]

60. Nadaf, N.Y.; Kanase, S.S. Biosynthesis of gold nanoparticles by *Bacillus marisflavi* and its potential in catalytic dye degradation. *Arab. J. Chem.* **2019**, *12*, 4806–4814. [CrossRef]

61. Sweeney, R.Y.; Mao, C.; Gao, X.; Burt, J.L.; Belcher, A.M.; Georgiou, G.; Iverson, B.L. Bacterial Biosynthesis of Cadmium Sulfide Nanocrystals. *Chem. Biol.* **2004**, *11*, 1553–1559. [CrossRef] [PubMed]

62. Bai, H.J.; Zhang, Z.M.; Guo, Y.; Yang, G.E. Biosynthesis of cadmium sulfide nanoparticles by photosynthetic bacteria *Rhodopseudomonas palustris*. *Colloids Surf. B Biointerfaces* **2009**, *70*, 142–146. [CrossRef] [PubMed]

63. Cui, R.; Liu, H.; Xie, H.; Zhang, Z.; Yang, Y.; Pang, D.; Xie, Z.; Chen, B.; Hu, B.; Shen, P. Living Yeast Cells as a Controllable Biosynthesizer for Fluorescent Quantum Dots. *Adv. Funct. Mater.* **2009**, *19*, 2359–2364. [CrossRef]

64. Suresh, A.K. Extracellular bio-production and characterization of small monodispersed CdSe quantum dot nanocrystallites. *Spectrochim. Acta Part A Mol. Biomol. Spectrosc.* **2014**, *130*, 344–349. [CrossRef] [PubMed]

65. Wu, S.; Su, Y.; Liang, R.; Ai, X.; Qian, J.; Wang, C.; Chen, J.; Yan, Z. Crucial factors in biosynthesis of fluorescent CdSe quantum dots in Saccharomyces cerevisiae. *RSC Adv.* **2015**, *5*, 79184–79191. [CrossRef]

66. Yamaguchi, T.; Tsuruda, Y.; Furukawa, T.; Negishi, L.; Imura, Y.; Sakuda, S.; Yoshimura, E.; Suzuki, M. Synthesis of CdSe Quantum Dots Using *Fusarium oxysporum*. *Materials* **2016**, *9*, 855. [CrossRef]

67. Kimber, R.L.; Lewis, E.A.; Parmeggiani, F.; Smith, K.; Bagshaw, H.; Starborg, T.; Joshi, N.; Figueroa, A.I.; van der Laan, G.; Cibin, G.; et al. Biosynthesis and Characterization of Copper Nanoparticles Using *Shewanella oneidensis*: Application for Click Chemistry. *Small* **2018**, *14*, 1703145. [CrossRef]

68. Jha, A.K.; Prasad, K.; Kulkarni, A.R. Synthesis of Gd_2O_3 nanoparticles using *Lactobacillus* sp.: A novel green approach. *Int. J. Green Nanotechnol. Phys. Chem.* **2010**, *2*, 31–38. [CrossRef]

69. Yeary, L.W.; Ji-Won, M.; Love, L.J.; Thompson, J.R.; Rawn, C.J.; Phelps, T.J. Magnetic properties of biosynthesized magnetite nanoparticles. *TMAG* **2005**, *41*, 4384–4389. [CrossRef]

70. Smeaton, C.M.; Fryer, B.J.; Weisener, C.G. Intracellular Precipitation of Pb by *Shewanella putrefaciens* CN32 during the Reductive Dissolution of Pb-Jarosite. *Environ. Sci. Technol.* **2009**, *43*, 8086–8091. [CrossRef]

71. Liu, C.; Liu, C.; Yen, J.; Yen, J. Characterization of lead nanoparticles formed by *Shewanella* sp. KR-12. *J. Nanopart. Res.* **2016**, *18*, 1–10. [CrossRef]

72. Priyanka, U.; Akshay, G.; Elisha, M.; Surya, T.; Nitish, N.; Raj, M. Biologically synthesized PbS nanoparticles for the detection of arsenic in water. *Int. Biodeterior. Biodegrad.* **2017**, *119*, 78–86.

73. Zhang, H.; Hu, X. Rapid production of Pd nanoparticle by a marine electrochemically active bacterium *Shewanella* sp. CNZ-1 and its catalytic performance on 4-nitrophenol reduction. *RSC Adv.* **2017**, *7*, 41182–41189. [CrossRef]

74. Cui, J.; Zhu, N.; Kang, N.; Ha, C.; Shi, C.; Wu, P. Biorecovery mechanism of palladium as nanoparticles by *Enterococcus faecalis*: From biosorption to bioreduction. *Chem. Eng. J.* **2017**, *328*, 1051–1057. [CrossRef]

75. Martins, M.; Mourato, C.; Sanches, S.; Noronha, J.P.; Crespo, M.T.B.; Pereira, I.A.C. Biogenic platinum and palladium nanoparticles as new catalysts for the removal of pharmaceutical compounds. *Water Res.* **2017**, *108*, 160–168. [CrossRef]

76. Konishi, Y.; Ohno, K.; Saitoh, N.; Nomura, T.; Nagamine, S.; Hishida, H.; Takahashi, Y.; Uruga, T. Bioreductive deposition of platinum nanoparticles on the bacterium *Shewanella algae*. *J. Biotechnol.* **2007**, *128*, 648–653. [CrossRef]

77. Jha, A.K.; Prasad, K.; Prasad, K. Biosynthesis of Sb_2O_3 nanoparticles: A low-cost green approach. *Biotechnol. J.* **2009**, *4*, 1582–1585. [CrossRef]

78. Jha, A.K.; Prasad, K.; Kulkarni, A.R. Synthesis of TiO_2 nanoparticles using microorganisms. *Colloids Surf. B Biointerfaces* **2009**, *71*, 226–229. [CrossRef]

79. Bansal, V.; Rautaray, D.; Ahmad, A.; Sastry, M. Biosynthesis of zirconia nanoparticles using the fungus *Fusarium oxysporum*. *J. Mater. Chem.* **2004**, *14*, 333–335. [CrossRef]

80. Zhang, D.; Tang, D.; Yamamoto, T.; Kato, Y.; Horiuchi, S.; Ogawa, S.; Yoshimura, E.; Suzuki, M. Improving biosynthesis of AuPd core-shell nanoparticles through Escherichia coli with the assistance of phytochelatin for catalytic enhanced chemiluminescence and benzyl alcohol oxidation. *J. Inorg. Biochem.* **2019**, *199*, 110795. [CrossRef]

81. Wang, C.; Lum, A.; Ozuna, S.; Clark, D.; Keasling, J. Aerobic sulfide production and cadmium precipitation by Escherichia coli expressing the *Treponema denticola* cysteine desulfhydrase gene. *Appl. Microbiol. Biotechnol.* **2001**, *56*, 425–430. [CrossRef] [PubMed]

82. Zhang, D.; Yamamoto, T.; Tang, D.; Kato, Y.; Horiuchi, S.; Ogawa, S.; Yoshimura, E.; Suzuki, M. Enhanced biosynthesis of CdS nanoparticles through *Arabidopsis thaliana* phytochelatin synthase-modified Escherichia coli with fluorescence effect in detection of pyrogallol and gallic acid. *Talanta* **2019**, *195*, 447–455. [CrossRef] [PubMed]

83. Gurunathan, S.; Kalishwaralal, K.; Vaidyanathan, R.; Venkataraman, D.; Pandian, S.R.K.; Muniyandi, J.; Hariharan, N.; Eom, S.H. Biosynthesis, purification and characterization of silver nanoparticles using *Escherichia coli*. *Colloids Surf. B Biointerfaces* **2009**, *74*, 328–335. [CrossRef] [PubMed]

84. Deljou, A.; Goudarzi, S. Green Extracellular Synthesis of the Silver Nanoparticles Using Thermophilic Bacillus Sp. AZ1 and its Antimicrobial Activity against Several Human Pathogenetic Bacteria. *Iran. J. Biotechnol.* **2016**, *14*, 25–32. [CrossRef] [PubMed]